Earthquakes and Structures, Vol. 4, No. 2 (2013) 203-217
DOI: http://dx.doi.org/10.12989/eas.2013.4.2.203

Damping identification procedure for linear systems: mixed numerical-experimental approach

Hazem Hossam El-Anwar, Mohammed Hassanien Serror*
and Hesham Sobhy Sayed

Dept. of Structural Engineering, Cairo University, Egypt

(Received January 12, 2012, Revised February 18, 2012, Accepted March 29, 2012)

Abstract. In recent decades, it has been realized that increasing the lateral stiffness of structure subjected to lateral loads is not the only parameter enhancing safety or reducing damage. Factors such as ductility and damping govern the structural response due to lateral loads. Despite the significant contribution of damping in resisting lateral loads, especially at resonance, there is no accurate mathematical representation for it. The main objective of this study is to develop a damping identification procedure for linear systems based on a mixed numerical-experimental approach, assuming viscous damping. The proposed procedure has been applied to a laboratory experiment associated with a numerical model, where a hollow rectangular steel cantilever column, having three lumped masses, has been fixed on a shaking table subjected to different exciting waves. The modal damping ratio has been identified; in addition, the effect of adding filling material to the hollow specimen has been studied in relation to damping enhancement. The results have revealed that the numerically computed response based on the identified damping is in a good fitting with the measured response. Moreover, the filling material has a significant effect in increasing the modal damping.

Keywords: damping identification; linear system; shaking table; steel tube; filling material

1. Introduction

System identification (SI) techniques play an important role in investigating and reducing gaps between the constructed structural systems and their structural design models, and in structural health monitoring for damage detection. A great amount of research has been conducted in SI (Inman 1989, Gawronski 2004, Adams 2007, Takewaki 2009, Takewaki *et al.* 2011). Modal-parameter SI and physical-parameter SI are two major branches in SI. The former is appropriate for identifying the overall mechanical properties of a structural system and exhibits stable characteristics in implementation. While the latter is important from different viewpoints, such as enhancement of reliability in active controlled structures or base-isolated structures, and its development is limited due to the requirement of multiple measurements or the necessity for complicated manipulation (Gawronski 2004, Takewaki 2009). A mixed approach is often used in

*Corresponding author, Assistant Professor, E-mail: mhassanien@cosmos-eng.com

which physical parameters are identified from the modal parameters obtained by the modal-parameter SI. However, a sufficient number of modal parameters must be obtained for the unique and accurate identification of the physical parameters.

Damage of building structures during sever earthquake ground motions results mainly from the resonance of the fundamental natural frequency of the building structures with the predominant frequency of the input motions. Although the damping has a significant contribution in mitigating the damage through controlling the structural response, yet there is no accurate mathematical representation for it. Moreover, it does not appear that damping identification techniques have been developed sufficiently. The difficulty in identifying the damping arises from the fact that energy is dissipated in the system through various mechanisms such as: viscous, friction, material, particle and hysteretic damping. Therefore, it might be useful to determine the damping experimentally or from pre-measured response for existing structures.

Takewaki and Nakamura (2000) adopted a new method of physical-parameter SI for shear building models. The story stiffness, the linear hysteretic damping ratio and the viscous damping coefficient in a specific story have been identified uniquely and simultaneously in a unified manner when the acceleration records at the floor just above and below the target story are available. Nilson *et al.* (2004) utilized procedures based on results of computational simulations of finite element models and experimental procedures based on modal analysis. Adams (2007) identified the changes in stiffness and damping forces as a function of frequency and damage level. The time domain model was introduced assuming that all of the mass, damping and stiffness parameters were known beforehand. Only then can the model be used to study the free and forced response to enable health monitoring of the component and to identify loading or damage. Curadelli *et al.* (2008) introduced a scheme to detect structural damage by means of the instantaneous damping coefficient identification using a wavelet transform. Parameters that characterize structural damping are used as damage-sensitive system properties. George and Dimitri (2009) extended their modal damping identification model for classically damped linear building frames to the non-classically damped case. Marco *et al.* (2009) introduced a method for estimating the elastic and dissipative parameters of composite plates through a mixed numerical-experimental identification procedure. Hann *et al.* (2009) combined the low resolution displacement measured by a GPS device and the high resolution acceleration measured by accelerometers to determine the stiffness of nonlinear single degree of freedom structures. Rajab and Okabayashi (2011) applied the subspace stochastic realization theories to a real bridge for estimating its dynamic characteristics under ambient vibration. A numerical simulation was carried out using a white noise excitation. The estimates obtained from this simulation are compared with those obtained from the finite element analysis, demonstrating good agreement. Moustafa (2011) developed a new framework for modeling design earthquake loads for inelastic structures. The ground acceleration is expressed as a Fourier series, with unknown amplitude and phase angle, modulated by an envelope function. An inverse dynamic problem is solved to obtain the ground acceleration, so that the structure performance is minimized.

2. Problem statement

In this study, a damping identification procedure has been proposed based on a mixed numerical-experimental approach. The analytical and measured dynamic responses are compared in order to identify the damping ratio through minimizing an objective function (Sayed 1998). The focus, in this paper, is directed towards testing the proposed procedure to identify the viscous damping behavior which is usually one of the unknown properties of the material and structures. Consequently, a linear system has been adopted to decouple the material damping, associated with the hysteretic behavior, from the viscous damping.

In order to examine the proposed procedure, a laboratory experiment has been conducted in association with a numerical model. A specimen of hollow rectangular steel cantilever column, having three lumped masses, has been considered. In order to enhance the system damping, different types of filling material can be added to the hollow specimen (Karunarathne 2001, Tu and Wang 2010). In this study, damping enhancement is based on filling the hollow specimen with a mixture of both sand and oil (300 ml oil per 1000 ml sand). This mixture is appropriate for the scale of specimen used in this study (tube profile in mm: 100 x 40 x 1). It is anticipated that viscosity and friction of this mixture shall be activated during specimen vibration, dissipating portions of the applied energy. It is worth noting that using concrete as a filling material (composite specimen) can be a valid option; however, an appropriate scaling for the specimen should be adopted and the modified stiffness should also be identified.

Beyond the scope of this paper, the same identification procedure shall be applied to a nonlinear system, including the hysteretic damping. A kinematic hardening with Von Mises yield criterion shall be adopted for steel material and Draker Prager yield criterion with multi-yield-surface shall be adopted for the sand-oil mixture. Hence, a damage index can then be correlated with the identified damping.

3. Proposed damping identification procedure

Herein, the system identification technique shall utilize: numerical model, measured excitation and measured response in order to identify the modal damping ratios for the used frequencies. The numerical model is made of two modules; the first is to solve the forward problem and the second is to solve the inverse problem. The forward problem obtains the structure response knowing the input excitation and the dynamic properties of the model. The inverse problem utilizes an optimization technique to search for the required dynamic properties that reduce the differences between the measured and computed response. In this study, a mixed numerical-experimental approach is used to identify the damping characteristics. The procedure can be summarized as follows:

1. Executing an experiment to measure the structural response for a given input excitation. The measured response is then digitized, filtered and analyzed
2. Applying Fast Fourier Transform (FFT) to the measured response in order to obtain the natural frequencies of the system. This will help in validating the numerical model.
3. Applying the decay of motion technique to the measured response to estimate the modal damping value that can be used as initial assumption in solving the inverse problem.
4. Applying the numerical model (Sayed 2002) to obtain the required damping properties using the estimated values from 2 and 3 as initial values.

3.1 Experiment setup

In this study, a shaking table (MTS 2011) is used to generate and apply the input excitation wave.

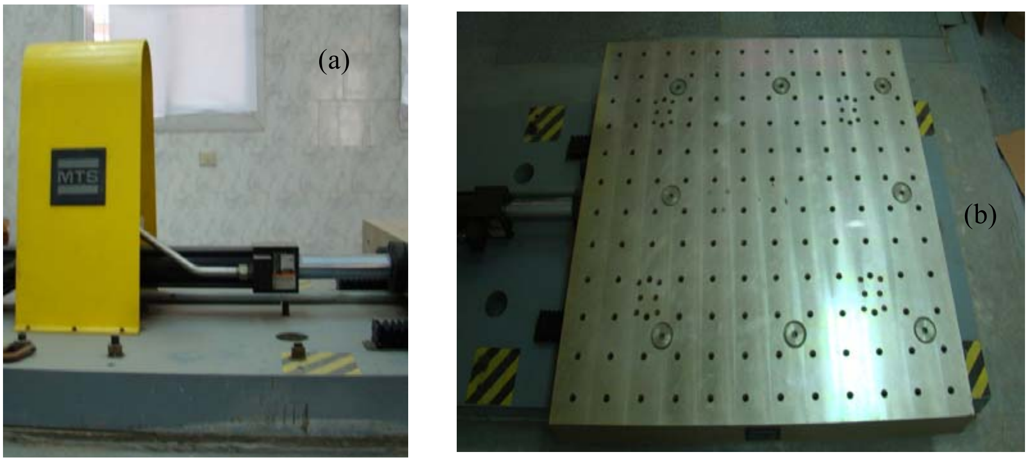

Fig. 1 Shaking table components: (a) Uniaxial actuator and (b) fixation table

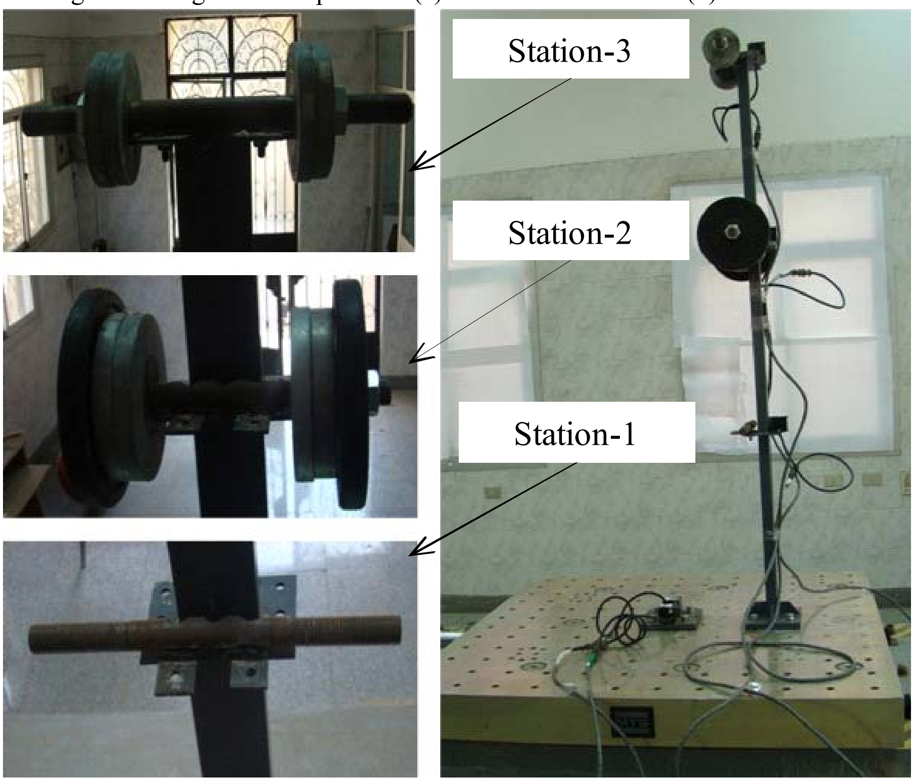

Fig. 2 The model specimen (cantilever steel tube) fixed on the shaking table, it has three lumped masses and data acquisition system installed at the target stations

Fig. 1 shows the components of the device. The table has a surface area of 1.5 m x 1.5 m and applies uniaxial excitation with a frequency range of 0-25 Hz.

Fig. 2 shows a real shot for the model specimen, which is a hollow rectangular (tube) steel section of 0.1 m x 0.04 m x 0.001 m (length x width x thickness). The steel grade is ST-37/2 with an ultimate strength of 3.6 t/cm^2 and a yield strength of 2.4 t/cm^2. The steel tube has been designed as a cantilever column with a total height of 2 m. Three plates, associated with three rods, have been welded at the levels: +0.66 m, +1.33 m and +1.98 m from the base level, namely: station-1, 2 and 3. These stations represent the locations where lumped masses are added and vibration responses are recorded. Hence, the specimen is almost representing a three-degree-of-freedom system. The lumped masses have been designed so that the natural frequencies of, at least, the first and second modes of vibration are within the frequency range of the shaking table (0-25 Hz). The three masses at the three stations, from station-1 to station-3, are: 4 kg, 34 kg and 12 kg, respectively, including the mass of all associated devices at the station. Damping of the specimen is enhanced through filling the tube with the sand-oil mixture.

Single-axis accelerometers of FBA ES-U (kinematics 2011) are used to record the input excitation and the response of the specimen. Generally, four accelerometers have been employed: three of them have been fixed at the three stations, and the fourth has been fixed on the shaking table itself to record the input excitation. For each input excitation, the experiment has been conducted twice with: (1) hollow specimen and (2) filled specimen.

3.2 Numerical model

Modal models of structures are the numerical models expressed in modal coordinates (Gawronski 2004). A modal matrix is used to introduce a new variable called modal displacement, z. The purpose of the numerical model is to define the modal damping ratio knowing the modal dynamic characteristics of the specimen (mass and stiffness) and the measured response against base excitation.

The forward problem is governed by the following classical equation of motion

$$\mathbf{M}\,\ddot{u} + \mathbf{C}\,\dot{u} + \mathbf{K}\,u = f \tag{1}$$

where M, C and K are mass, damping and stiffness matrices respectively, f and u are excitation and displacement response vectors respectively, and $(\dot{\ })$ denotes differentiation with respect to elapsed time. Herein, modal damping is used by decoupling the system using a pre-determined number of mode shapes. The matrix of mode shapes, modal matrix, ($\mathbf{\Phi}$) is used to decouple the system as follows

$$\mathbf{m}\,\ddot{z} + \mathbf{c}\dot{z} + \mathbf{k}z = p \tag{2}$$

where $\mathbf{m} = \Phi^T \mathbf{M}\,\Phi$ is the modal mass matrix, $\mathbf{c} = \Phi^T \mathbf{C}\,\Phi$ is the modal damping matrix, $\mathbf{k} = \Phi^T \mathbf{K}\,\Phi$ is the modal stiffness matrix, $p = \Phi^T f$ is the load vector, and z is the generalized degrees of freedom, modal displacement, where $u = \Phi\ z$. Given the modal mass and stiffness and the initial conditions for the structure together with initially estimated (assumed) modal damping, Eq. (2) can then be solved for an excitation using Newmark method of integration.

The modal damping ratios are then the *model parameters* to be determined through the proposed system identification procedure. The model parameters can be identified using the set of measurements for the structure response against base excitations. Consequently the model parameters ($\rho_i = diagonal[c]$) can be identified by minimizing the error function (objective function) $G(\rho_i)$ that is stemmed from the least square approach by summing the square of the errors between measured and identified structure deformations as follows (Sayed 2002)

$$G(\rho_i) = \sum_{n=1}^{n=NOST} \sum_{t=0}^{T} (u_l - u_l^m)(u_l - u_l^m) \tag{3}$$

where the superscript (^{m}) denotes measured values of deformation, *NOST* denotes the total number of stations at which the structure deformation are measured, and *T* is the total number of discrete time steps. In order to minimize the objective function, nonlinear unconstrained optimization technique is usually used. Consequently, gradients of the objective function with respect to the model parameters are required. Differentiating Eq. (3), the following expressions can be obtained

$$\frac{\partial G}{\partial \rho_i} = 2 \sum_{n=1}^{n=NOST} \sum_{t=0}^{T} (u_l - u_l^m) \frac{\partial u_l}{\partial \rho_i} = 2 \sum_{n=1}^{n=NOST} \sum_{t=0}^{T} (u_l - u_l^m) \phi_{lk} \eta_{ki} \tag{4}$$

$$\frac{\partial^2 G}{\partial \rho_i \partial \rho_j} = 2 \sum_{n=1}^{n=NOST} \sum_{t=0}^{T} \{(u_l - u_l^m) \frac{\partial^2 u_l}{\partial \rho_i \partial \rho_j} + \frac{\partial u_l}{\partial \rho_i} \frac{\partial u_l}{\partial \rho_j}\} = 2 \sum_{n=1}^{n=NOST} \sum_{t=0}^{T} \{(u_l - u_l^m) \phi_{lk} \xi_{kij} + \phi_{lk} \phi_{lr} \eta_{ki} \eta_{rj}\} \tag{5}$$

where $\eta_{jki} = z_{k,i}$ *and* $\xi_{kij} = z_{k,ij}$ are the first and second derivatives of the modal generalized response (z_j) with respect to the model parameters (ρ_i or ρ_j).

The convergence is achieved when the updated values of the parameters differ from the previous values by a predetermined error margin. The unconstrained optimization reveals the optimal values of the parameters that give minimal value for the objective function.

In order to determine the structure modal dynamic characteristics: mass and stiffness, a general purpose finite element program (SAP 2000) is used. Moreover, the same program is used to determine the structure frequencies and mode shapes (Φ) required in the analysis. The generated finite element model uses frame elements to model a hollow rectangular steel cantilever column fixed at the base, inheriting the geometry, material and boundary conditions of the specimen. A mass element has been utilized to represent the lumped masses at the three stations along specimen height. The boundary conditions have been defined using a base excitation as acceleration time history function equal to that recorded by the accelerometer fixed on the shaking table. The resulted natural frequencies are 2.9 Hz and 17 Hz for the first and second modes of vibration, respectively. The third mode of vibration has a frequency of 77.9 Hz, which is out of the frequency range of the shaking table.

3.3 Input excitation

Four waves have been selected for excitation: Sweep1, Sweep2, Kobe earthquake and Loma Prieta earthquake. Table 1 lists the earthquake record information. The selection criterion is to examine the excitation of both the artificial time history and the real earthquake time history. The artificial time history can be chosen to have a specific frequency content that can excite a specific vibration mode of the system. The real earthquake time history, however, has its own inherited frequency content. The selected records for Kobe and Loma Prieta earthquakes are sample records which afford the same frequency content that is capable to excite the system in its modes of vibration. The PGA of both records has been scaled up and down in order to apply appropriate excitation to the specimen, maintaining its behavior within the linear elastic range.

The acceleration time history for earthquakes is used as given in the official web site of the Pacific Earthquake Engineering Research center (PEER 2011). The main characteristics of Kobe

Table 1 Earthquake record information (PEER 2012)

Earthquake	Station	Record/Component	Magnitude (M)	Epicentral distance (km)	HP (Hz)	LP (Hz)	PGA (g)	PGV (cm/s)	PGD (cm)
Kobe 1995/01/16 20:46	0 KJMA	KOBE/KJM-UP	6.90	18.27	0.05	null	0.343	38.3	10.29
Loma Prieta 1989/10/18 00:05	1678 Golden Gate Bridge	LOMAP/GGB-UP	6.93	100.19	0.2	30	0.056	11.3	3.81

earthquake are: peak ground acceleration (PGA) of 0.343 g, time increment of 0.02 sec and wave duration of 48 sec. The acceleration time history has been scaled to 70% in order to keep the behavior of the system in the elastic range. The main characteristics of Loma Prieta earthquake are: peak ground acceleration (PGA) of 0.056 g, time increment of 0.005 sec and wave duration of 40 sec. The acceleration time history has been scaled to 500% in order to have a significant excitation to the system within the elastic range.

The Sweep excitation is a wave that includes a certain range of frequencies. The test starts with an initial frequency that increases with a constant rate to an end frequency within a period of time. Sweep1 test starts with a frequency 1 Hz that increases with a constant rate to 10 Hz within 60 sec. Sweep2 test starts with a frequency 10 Hz that increases with a constant rate to 20 Hz within 20 sec. It is worth noting that the frequency range of Sweep1 and Sweep2 tests has been selected so that it spans the numerically obtained first mode frequency (2.9 Hz) and the second mode frequency (17 Hz), respectively.

Fig. 3 shows the acceleration time history and the frequency content of the four selected waves. For Sweep1 and Sweep2 tests the amplitude of the acceleration increases with time. The reason for this pattern is that for low frequencies the displacement corresponding to the input acceleration is relatively large as compared to the displacements determined at large frequencies. In order to guarantee elastic behavior of the system at low frequencies and at the same time achieve significant displacement values that can be applied to the shaking table at high frequencies, a pattern of increasing acceleration amplitude has been employed.

4. Results and discussion

The proposed identification procedure and the associated results have been summarized as follows:

4.1 Data filtering

Filtering has been applied to the recorded raw data in order to remove both the DC shift and noise. The noise has been removed through Hanning filter. Fig. 4 shows a filtration sample for an acceleration record at Station-3 during Sweep1 test.

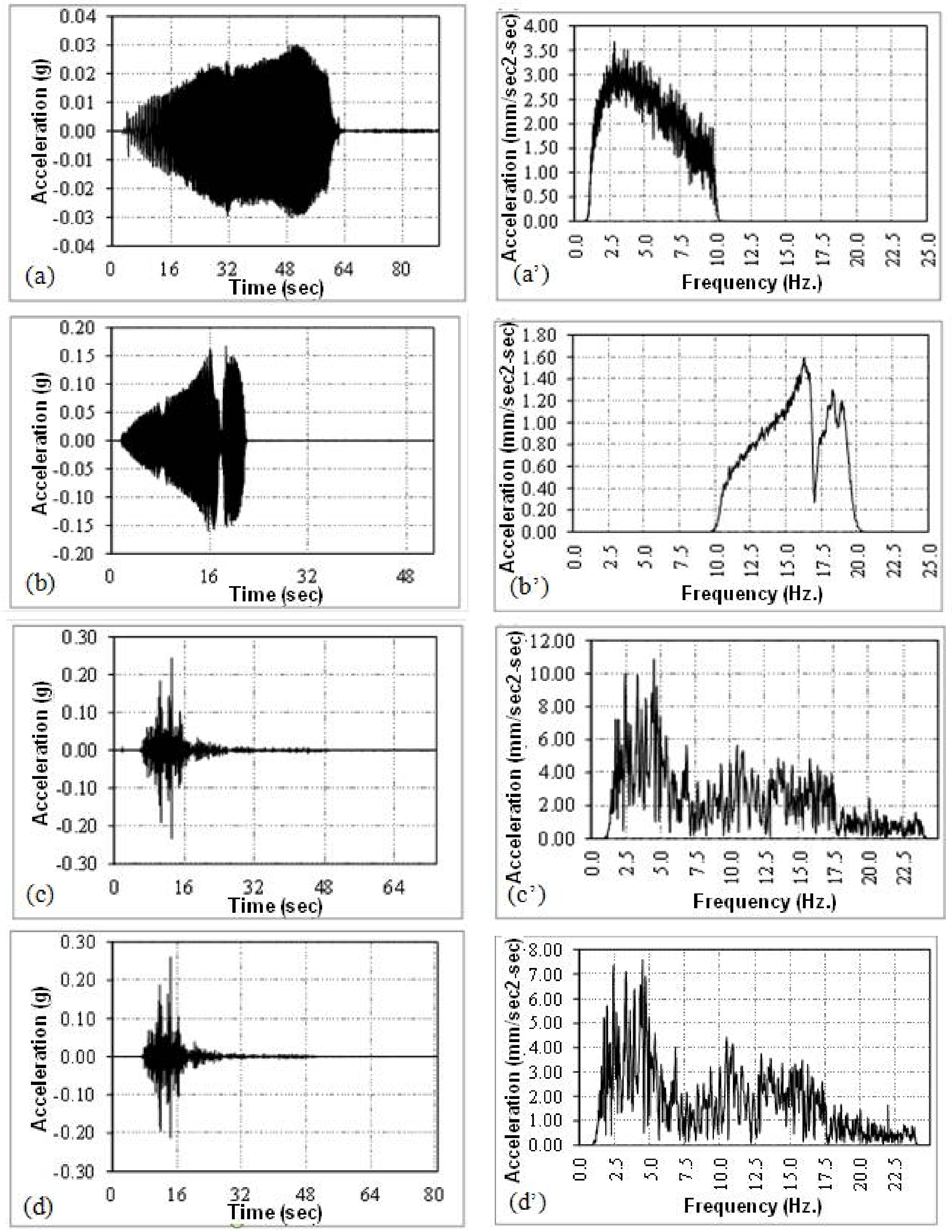

Fig. 3 Acceleration time history and frequency content for four selected input excitations: (a) Sweep1, (b) Sweep2, (c) Kobe earthquake and (d) Loma Prieta earthquake

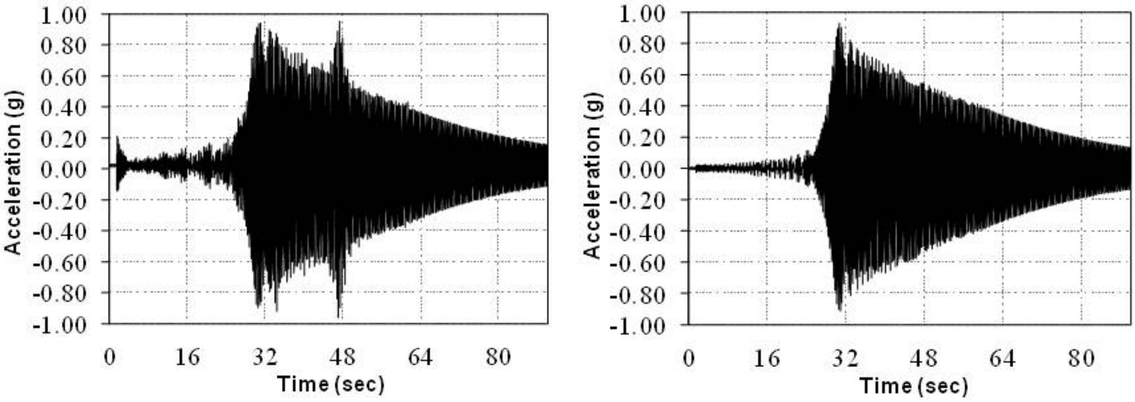

Fig. 4 A filtration sample for an acceleration record at station-3 during Sweep1 test: (a) Raw data and (b) filtered data

4.2 Fast Fourier Transformation (FFT)

Upon filtering the recorded data, Fast Fourier Transformation (FFT) has been performed to transform results from the time domain to the frequency domain. The purpose of FFT is to identify the natural frequencies of the system, based on the experimental records, in order to validate the numerical finite element model.

Fig. 5 shows the response at Station-3 in the frequency domain. It compares the response for the four exciting waves for the cases of hollow and filled specimen. The peaks shown in Fig. 5. indicate the natural frequencies of the system. The frequency content for Sweep1 test (1-10 Hz) affords only one peak at the first mode of vibration (see Fig. 5(a)); similarly, the frequency content for Sweep2 test (10-20 Hz) affords also one peak, however, at the second mode of vibration (see Fig. 5(b)). For Kobe and Loma Prieta earthquakes (see Figs. 5(c) and 5(d)), the frequency content includes both modes of vibration; hence, two peaks are observed. It is obvious from Figs. 5c and 5d that the contribution of the second mode of vibration is almost negligible compared with the first mode. Hence, the dynamic properties identified by these two earthquakes shall be considered representative for the first mode only. Table 2 summarizes the numerically and experimentally obtained natural frequencies of the system.

4.3 Damping initial estimation based on the decay of motion

The Decay of motion technique focuses on the free vibration phase of the displacement response. At this phase, the displacement decays exponentially; and hence, the damping ratio can be calculated. Table 3 summarizes the initially estimated damping ratio of the system by applying the decay of motion technique to the measured displacement response at Station-3. The damping ratio has been calculated for the four exciting waves based on two cases of specimen: hollow and filled tubes. It is worth noting that the identification based on Sweep1, Kobe and Loma Prieta shall be considered representative for the first mode of vibration; meanwhile, the identification based on Sweep 2 shall be considered representative for the second mode of vibration. The damping ratio associated with the first mode of vibration can be calculated as the average of the results obtained

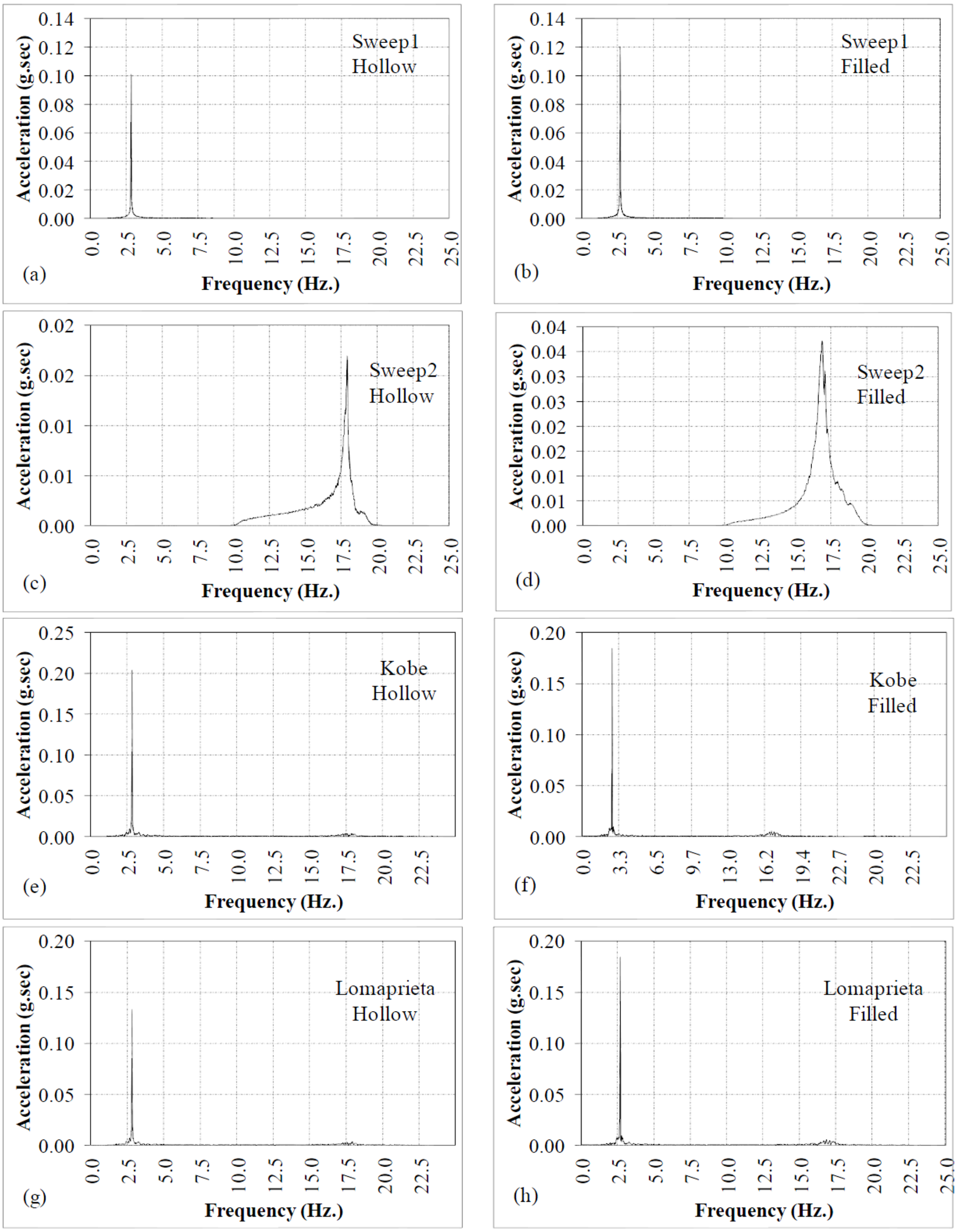

Fig. 5 Acceleration response at station-3 in the frequency domain: (a) Sweep1 Hollow test; (b) Sweep1 Filled test; (c) Sweep2 Hollow test; (d) Sweep2 Filled test; (e) Kobe Hollow test; (f) Kobe Filled test; (g) Loma Prieta Hollow test and (h) Loma Prieta Filled test

Table 2 Analytically and experimentally obtained natural frequencies (Hz.) of model specimen

Test	Hollow tube		Filled tube	
	Mode 1	Mode 2	Mode 1	Mode 2
Sweep1	2.86	N.A.	2.69	N.A.
Sweep2	N.A.	17.90	N.A.	16.85
Kobe	2.85	N.A.	2.69	N.A.
Loma Prieta	2.84	N.A.	2.69	N.A.
FEM Model	2.86	17.91	2.7	16.9

Table 3 Initially estimated damping ratio of the model specimen based on the decay of motion technique

Test	Vibration mode	Hollow tube				Filled tube			
		U_i	U_{i+j}	j	ξ%	U_i	U_{i+j}	j	ξ%
Sweep1	1	4.26	4.78	10	0.185	4.38	5.03	10	0.218
Sweep2	2	0.031	0.036	10	0.247	0.013	0.017	10	0.422
Kobe	1	7.83	8.98	10	0.219	7.06	8.30	10	0.258
Loma Prieta	1	4.24	4.78	10	0.19	6.92	8.14	10	0.258

Table 4 Identified damping ratio (%)

Test	Vibration mode	Hollow tube	Filled tube
Sweep1	1	0.154	0.219
Sweep2	2	0.350	0.600
Kobe	1	0.153	0.202
Loma Prieta	1	0.156	0.202

Table 5 Modal damping enhancement upon adding the filling material

Modal damping	Hollow tube	Filled tube	Damping enhancement
ξ1 average (%)	0.155	0.210	35.5%
ξ2 average (%)	0.350	0.600	74.4%

from Sweep1 test and Kobe and Loma Prieta earthquakes. It equals 0.198% and 0.245% for hollow and filled specimens, respectively. On the other hand, the damping ratio associated with the second mode of vibration is calculated from Sweep2 test. It equals 0.247% and 0.422% for hollow and filled specimens, respectively.

4.4 *Mixed numerical-experimental identified damping*

Given the specimen geometry, material, masses and boundary conditions, the finite element model is generated and the modal dynamic characteristics are computed: shape of vibration, mass, stiffness, participation factor, and vibration frequency. Given the modal dynamic characteristics and the assumed modal damping of specimen, the numerical model is then analyzed in Eq. (2) to compute the response: acceleration, velocity and displacement for each input excitation.

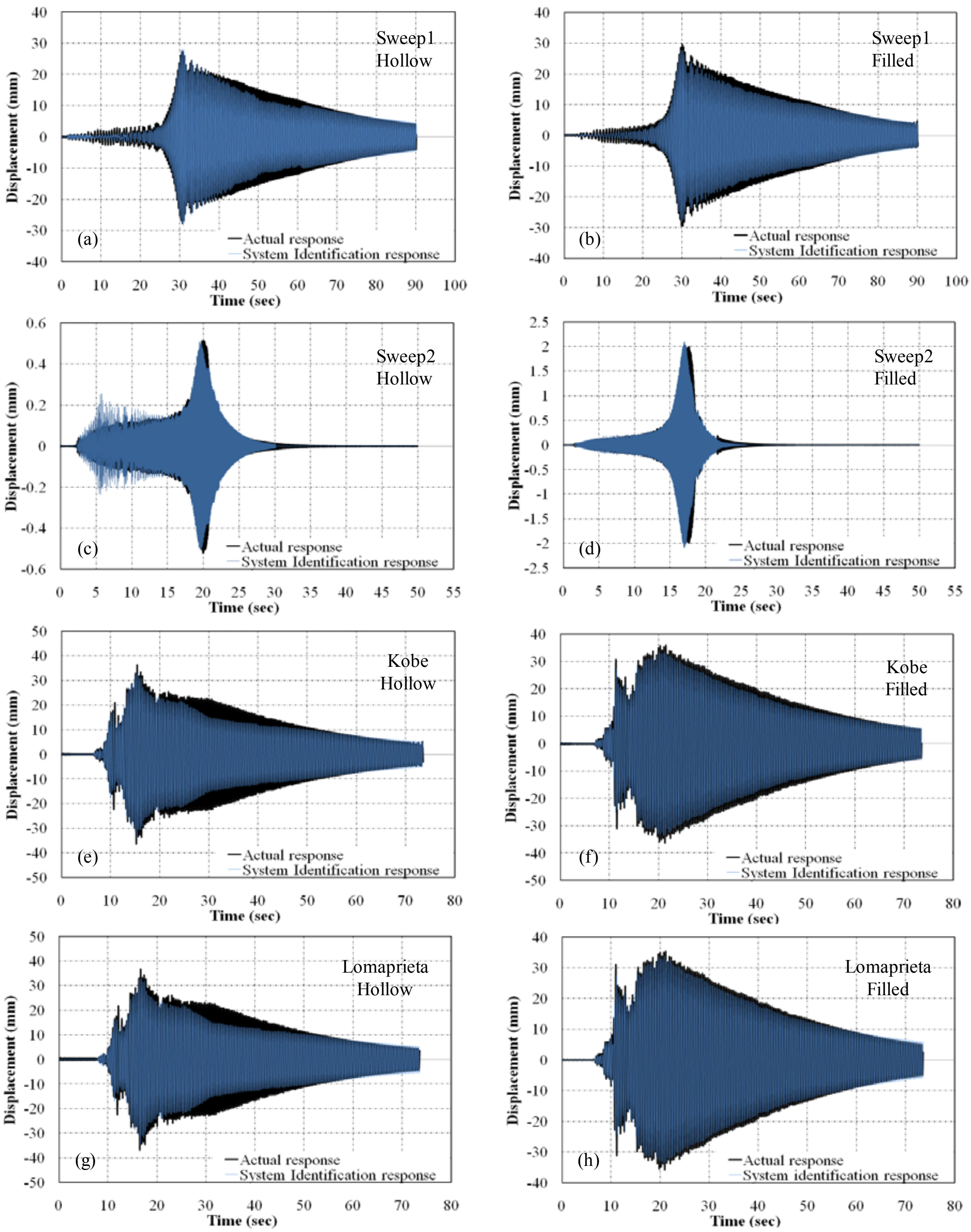

Fig. 6 Comparison between measured and computed response at station-3: (a) Sweep1 Hollow test; (b) Sweep1 Filled test; (c) Sweep2 Hollow test; (d) Sweep2 Filled test; (e) Kobe Hollow test; (f) Kobe Filled test; (g) Loma Prieta Hollow test and (h) Loma Prieta Filled test

The equation that governs the assumed damping ratio and indicates its accuracy is called the objective function $G(\rho)$ as given in Eq. (3), representing the difference between numerical and experimental responses. Newton method of optimization has been employed to minimize the objective function and to obtain the modal damping ratio of the system. The numerical model is then reanalyzed in Eq. (2) using the identified damping to compute the comparable response.

Fig. 6 shows a comparison between the measured displacement response at Station-3 and the numerically computed response, at the same station, based on the identified damping ratio. It is obvious that both responses have almost the same pattern; meanwhile, there is a slight difference in the amplitude. Table 4 summarizes the identified values of damping ratio. The damping ratio associated with the first mode of vibration can be determined as the average of the results obtained from Sweep1 test and Kobe and Loma Prieta earthquakes. It equals 0.155% and 0.210% for hollow and filled specimens, respectively. On the other hand, the damping ratio associated with the second mode of vibration is determined from Sweep2 test. It equals 0.350% and 0.600% for hollow and filled specimens, respectively.

Aside of the damping identification question, the results have also shown that the damping ratio of the system has been increased upon filling the tube with the sand-oil mixture. This can be foreseen as a passive control device in the system for energy dissipation. Table 5 summarizes the results of the damping ratios (ξ) and the enhancement obtained. The damping ratios of the first and second modes of vibration have been increased by 35.5% and 74.4%, respectively, upon adding the filling material. This increase is anticipated due to energy dissipation in sand friction and oil viscosity. It is worth noting that despite the increase in damping ratio of the system the filling material increases, in turn, the mass and consequently the seismic forces applied to the system. Therefore, the added mass and the increase in damping should be compromised in order to achieve the optimum response in presence of such control device.

5. Conclusions

In this study, a damping identification procedure has been proposed based on a mixed numerical-experimental approach. The analytical and measured dynamic responses are compared in order to identify the damping ratio through minimizing an objective function. The focus, in this paper, is directed towards testing the proposed procedure to identify the viscous damping behavior for a linear system. In order to examine the proposed procedure, a laboratory experiment has been conducted in association with a numerical model. A specimen of hollow rectangular steel cantilever column, having three lumped masses, has been considered. In addition, the effect of adding filling material to the hollow specimen has been studied in relation to damping enhancement.

The proposed procedure can be summarized in four main steps: (1) Filter the measured response to eliminate the DC shift and noise, (2) Apply the Fast Fourier Transformation to transform the measured response from the time domain to the frequency domain and then obtain the natural frequencies of the system, verifying the physical model against the numerical model, (3) Apply the decay of motion technique to the measured response to estimate the initial damping ratio of the system and (4) Apply the numerical model (Sayed 2002) to obtain the required damping properties through minimizing an objective function that represents the difference between the numerically and experimentally obtained responses.

The conclusions are summarized as follows:

1. The results have revealed that the computed response based on the proposed damping identification procedure is in a good fitting with the measured response.
2. Aside of damping identification, the results have also revealed that damping of the system has been increased upon filling the tube with the sand-oil mixture. This can be foreseen as a passive control device for energy dissipation. However, the added mass of filling material and the increase in damping should be compromised in order to achieve the optimum response in presence of such control device.

Beyond the scope of this paper, the same identification procedure shall be applied to a nonlinear system, including the hysteretic damping. A kinematic hardening with Von Mises yield criterion shall be adopted for steel material and Draker Prager yield criterion with multi-yield-surface shall be adopted for the sand-oil mixture. Hence, a damage index can then be correlated with the identified damping.

References

Adams, D. (2007), "Health monitoring of structural materials and components: Methods with applications", *John Wiley & Sons*, New York.

Curadelli, R.O., Riera, J.D., Ambrosini, D. and Amani, M.G. (2008), "Damage detection by means of structural damping identification", *Eng. Struct.*, **30**(12), 3497-3504.

Gawronski, W.K. (2004), "Advanced structural dynamics and active control of structures", *Springer*, Berlin.

George, A.P. and Dimitri, E.B. (2009), "On a modal damping identification model for non-classically damped linear building structures subjected to earthquakes", *Soil Dyn. Earthq. Eng.*, **29**(3), 583-589.

Hann, C.E., Singh-Levett, I., Deam, B.L., Mander, J.B. and Chase, J.G. (2009), "Real-time system identification of a nonlinear four-story steel frame structure-Application to structural health monitoring", *IEEE Sens. J.*, **9**(11), 1339-1346.

Inman, D. (1989), "Vibration: With control, measurement, and stability", *Prentice-Hall*, Englewood Cliffs, NJ.

Karunarathne, N. (2001-2002), "Damping of frame structures: An educational shake table test", *Student Research Accomplishments*, Multidisciplinary Center for Earthquake Engineering Research (MCEER).

Kinemetrics (2011), http://www.kinemetrics.com/p-163-Home.aspx.

Marco, M., Thomas, G., Joël, C. and Alain, S. (2009), "Numerical-experimental identification of the elastic and damping properties in composite plates", *Compos. Struct.*, **90**(2),180-187.

Moustafa, A. (2011), "Damage-based design earthquake loads for single-degree-of-freedom inelastic structures", *J. Struct. Eng.-ASCE*, **137**(3), 456-467.

MTS. (2011), http://www.mts.com/.

Nilson, B., Paulo, R.N. and Renato, B. (2004), **"**Experimental identification of damping", *Int. J. Solids Struct.*, **41**(13), 3585-3594.

PEER. (2012), Kobe record: http://peer.berkeley.edu/smcat/data/ath/KOBE/KJM-UP.AT2, Loma Prieta record: http://peer.berkeley.edu/smcat/data/ath/SANFRAN/GGP-UP.AT2.

Rajab, M. and Okabayashi, T. (2011), "System identification of highway bridges from ambient vibration using subspace stochastic realization theories", *Earthq. Struct.*, **2**(2), 189-206.

Sayed, H.S. (1998), "Modal damping identification for multi degrees of freedom dynamic systems", *J. Eng. Appl. Sci.*, **45**, 345-359.

Sayed, H.S. (2002), "Frequency domain modal damping identification for continuous systems: formulation and applications", *Civil Eng. Res. Mag.*, **24**.

Takewaki, I. and Nakamura, M. (2000), "Stiffness-damping simultaneous identification using limited

earthquake records", *Earthq. Eng. Struct. D.*, **29**(8), 1219-1238.
Takewaki, I. (2009), "Building control with passive dampers: Optimal performance-based design for earthquakes", *John Wiley and Sons Ltd,* 320.
Takewaki, I., Nakamura, M. and Yoshitomi, S. (2011), "System identification for structural health monitoring", *WIT Press*, 272.
Tu, Y. and Wang, G. (2010), "Damping parameter identification and study of metal foam filled steel tube", *J. Mater. Civil Eng.*, **22**(4), 397-402.
Uhl, T. (2007), "The inverse identification problem and its technical application", *Arch. Appl. Mech.*, **77**(5), 325-337.

IT